

1,4-Benzodiazepine-2,5-diones as small molecule antagonists of the HDM2–p53 interaction: discovery and SAR

Daniel J. Parks, Louis V. LaFrance,[†] Raul R. Calvo, Karen L. Milkiewicz,[‡] Varsha Gupta,[§] Jennifer Lattanze, Kannan Ramachandren, Theodore E. Carver, Eugene C. Petrella,^{||} Maxwell D. Cummings, Diane Maguire, Bruce L. Grasberger and Tianbao Lu*

Johnson & Johnson Pharmaceutical Research and Development, 665 Stockton Drive, Exton, PA 19341, USA

Received 14 September 2004; revised 2 November 2004; accepted 2 November 2004

Available online 18 November 2004

Abstract—A library of 1,4-benzodiazepine-2,5-diones was screened for binding to the p53-binding domain of HDM2 using ThermoFluor®, a miniaturized thermal denaturation assay. The hits obtained were shown to bind to HDM2 in the p53-binding pocket using a fluorescence polarization (FP) peptide displacement assay. The potency of the series was optimized, leading to sub-micromolar antagonists of the p53–HDM2 interaction.

© 2004 Elsevier Ltd. All rights reserved.

The p53 tumor suppressor protein plays a central role in the coordination of the cellular response to stress through the initiation of growth arrest and/or the induction of apoptosis.¹ The *p53* gene has been the subject of intense study since it was discovered that more than 50% of human cancers have mutations in this gene, and that abnormalities in this gene are among the most common molecular events correlated with neoplasia.² There are also instances of human cancers in which wild type p53 is present, but is inactivated through alternate means such as overexpression^{3,4} or amplification⁵ of *hdm2*.

The *hdm2* oncogene product (HDM2) suppresses the transcriptional activity of p53 in three ways: by direct binding to the *N*-terminal transactivation domain of

p53, exporting p53 from the nucleus into the cytoplasm and promoting its proteosomal degradation via ubiquitination through HDM2's E3 ligase activity.⁶

The disruption of the protein–protein interaction between p53 and HDM2 is an attractive approach for cancer therapy, because it offers the possibility to up-regulate the p53 response.⁷

Within the last few years there have been several reports of small molecule HDM2 antagonists, most of which are not very potent.^{8–11} Two recent reports describe more potent molecules.^{12,13} Herein we report the discovery and optimization of a series of 1,4-benzodiazepine-2,5-diones (BDPs) that act as potent antagonists of the HDM2–p53 interaction.

A library of BDPs was designed using Directed Diversity®,^{14–16} a suite of computational tools that can be used to analyze compound properties as part of the library design process. The library was synthesized utilizing the highly efficient and versatile Ugi four-component condensation reaction (Scheme 1).¹⁷ An anthranilic acid, an amine, an aldehyde, and 1-isocyanocyclohexene were combined, followed by acid-catalyzed cyclization, producing the desired BDPs in good yield and purity.^{18,19}

BDPs (22,000) produced in this way were screened with our proprietary ThermoFluor® screening technology.²⁰ The ThermoFluor® screening method is

Keywords: 1,4-Benzodiazepine-2,5-diones; p53; HDM2; ThermoFluor; Fluorescence polarization peptide displacement assay; p53–HDM2 interaction.

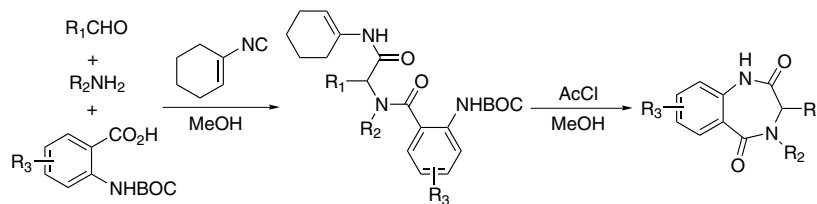
* Corresponding author. Tel.: +1 610 458 6068; fax: +1 610 458 8249; e-mail: tlu3@prduj.jnj.com

[†] Present address: GlaxoSmithKline, Inc., 1250 South Collegeville Rd, Collegeville, PA 19426-0989, USA.

[‡] Present address: Cephalon, Inc., 145 Brandywine Parkway, West Chester, PA 19380, USA.

[§] Present address: Helicon Therapeutics, Inc. 1 Bioscience Park Drive, Farmingdale, NY 11735, USA.

^{||} Present address: Suntory Pharmaceutical Research Laboratories LLC One Kendall Square, Bldg. 1400W Cambridge, MA 02139, USA.



Scheme 1. Ugi condensation reaction followed by cyclization.

a high-throughput, direct binding assay that measures the affinity of compounds toward a protein target (e.g., HDM2 (residues 17–125)). Hits are identified by a shift in T_m greater than three times the standard deviation ($\sim 0.2^\circ\text{C}$), at a standard concentration. By measuring the compound-dependent difference in protein melting temperature (T_m) at a series of compound concentrations, the dissociation constant (K_d) of that compound can be calculated.

A fluorescence polarization (FP) assay was used to characterize confirmed ThermoFluor[®] screening hits. The polarization of a fluorescein-labeled p53 peptide analog was measured by excitation at 485 nm and emission at 530 nm. The change in polarization upon displacement of the peptide from HDM2 (residues 17–125) by an antagonist was expressed as a percent with respect to the fluoresceinated peptide control.²¹

Most of the confirmed screening hits initially identified by ThermoFluor[®] belonged to a subset of the BDP library produced from α -amino esters as the amine component. A representative member is shown in Figure 1. Although the esters were consistent hits, their low solubility precluded screening in the FP assay, thus they were saponified to the acid yielding more soluble compounds.

Since the BDP acids derived from amino esters possessed two chiral centers, they were obtained as mixtures of diastereomers. Chromatographic separation typically afforded two compounds with dramatically different potencies (e.g., **1** and **2** in Table 1). The identity of the diastereomers was investigated using the parent BDP ester derived from the enantiomerically pure (*S*)-phenylglycine methyl ester. A series of NMR experiments in conjunction with molecular modeling established the active diastereomer as having the (*S,S*) configuration.²²

It was discovered that hydrolysis of the methyl esters resulted in epimerization of both chiral centers. The reported activities of the BDP acids therefore represent

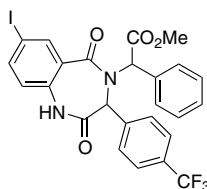
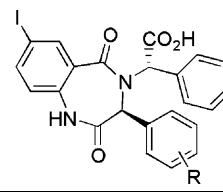


Figure 1. A representative BDP ester screening hit.

Table 1. SAR of 1,4-benzodiazepine-2,5-dione carboxylic acids: Optimization at position C-3



Compd	R	FP IC ₅₀ (μM)
1 ^a	4-CF ₃	31 ± 2
2	4-CF ₃	2.2 ± 0.3
3	H	38 ± 2
4	4-CH ₃	13.3 ± 0.6
5	4-CH ₂ CH ₃	7.5 ± 0.4
6	4-CH(CH ₃) ₂	18 ± 1
7	4-Cl	2.5 ± 0.4
8	4-OCF ₃	1.32 ± 0.05
9	2-CF ₃	>125
10	3-CF ₃	45 ± 3

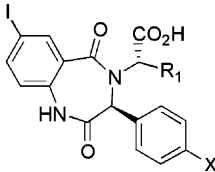
^a (*R,S*), (*S,R*) Racemic mixture.

the potency of the racemic mixture ((*S,S*) and (*R,R*)) of the most potent diastereomer. For example, the IC₅₀ value reported for **1** corresponds to the potency of the (*R,S*) and (*S,R*) mixture, and the IC₅₀ value reported for **2** corresponds to the potency of the (*R,R*) and (*S,S*) mixture.

The optimal substituent on the phenyl ring at C-3 was investigated (Table 1). The absence of a substituent resulted in a dramatic loss of potency as exemplified by **3**. Gradually increasing the alkyl substituent size in the *para*-position shows that an ethyl group is optimal for these substituents (**4–6**). Replacement with a chloro results in a compound equipotent to the CF₃ analog (**7**) while an OCF₃ group is slightly more potent (**8**). Substitution at either the *ortho*- or *meta*-positions results in a sharp loss in activity (**9** and **10**).

While maintaining the group at position C-3, substitution at the acid sidechain was explored. Commercially available α -amino esters were used directly, or the corresponding amino acids were converted to the methyl ester using HCl in methanol generated in situ by the careful addition of thionyl chloride to a methanol suspension of the amino acid.

When the α -amino acid was not commercially available, the α -amino ester hydrochloride was synthesized through a modified Strecker reaction.²³ The intermediate α -amino nitrile intermediate was converted directly to the α -amino ester by refluxing in HCl/methanol.

Table 2. SAR around the acid sidechain substituent


Compd	X	R ₁	TF <i>K</i> _d (μM)	FP IC ₅₀ (μM)	Compd	X	R ₁	TF <i>K</i> _d (μM)	FP IC ₅₀ (μM)
7	Cl		—	2.5 ± 0.4	18	Cl		—	0.67 ± 0.04
11	Cl		—	64 ± 5	19	Cl		14.3	16.5 ± 0.8
12	Cl		—	14 ± 1	20	Cl		0.067	0.42 ± 0.02
13	Cl		—	12.0 ± 0.3	21	Cl		0.083	0.62 ± 0.04
14	Cl		—	12 ± 1	22	CF ₃		—	0.62 ± 0.03
15	Cl		0.167	1.59 ± 0.09	23	OCF ₃		0.083	0.76 ± 0.09
16	Cl		0.083	1.55 ± 0.08	24	Cl		—	2.7 ± 0.1
17	Cl		—	2.27 ± 0.09	25	Cl		—	20 ± 1

The free base of the amino ester was formed prior to the Ugi condensation.

Some representative results are shown in Table 2. Replacement of the phenyl ring with a cyclohexyl group resulted in a dramatic loss of potency (**11**). This may be due to the greater steric bulk of the saturated ring or, more likely, a conformational effect that limits access to the conformation required for binding.

The acyclic derivatives **12** and **13** show that saturated groups are tolerated; however, they are not as good as a phenyl ring. The extra methyl group of **13** does not significantly enhance potency.

Insertion of a methylene between the *alpha*-carbon and the aryl ring leads to a >4-fold decrease in potency (**14** vs **7**). If the methyl is appended to the *para*-position however, a slight increase in potency is observed (**15**). Increasing the size to an isopropyl (**16**) does not significantly improve the potency and a *t*-butyl reverses the trend (**17**).

Incorporation of a CF₃- increases activity by nearly 4-fold (**18**) when compared to **7**. This suggests that the hydrophobicity of the 4-substituent is important, which is corroborated by the activity of **19** with a polar hydroxy group in the 4-position. Another factor that affects the binding may be the shape of the *para*-substituent. Methyl and trifluoromethyl groups are essentially spherical while the isopropyl group is obviously not. Other spherically symmetrical substituents are the halogens:

chloro- and bromo- (**19** and **20**) and show the greatest binding affinity, with the smaller chloro-group being slightly better.

Compounds **18**, **20**, and **21** represent the first compounds of the BDP series to achieve sub-micromolar activity. Other compounds that also showed nanomolar activity include those in which the 4-ClPh ring at position C-3 was replaced by a 4-CF₃Ph or 4-CF₃OPh group (**22** and **23**, respectively).

Substitution at the *meta*-position (**24**) does not drastically affect potency (cf. **23** and **7**), whereas *ortho*-substitution is not tolerated (**25**).

In an attempt to lower the molecular weight of the compounds, replacements for the iodo-group were investigated (Table 3). The removal of the iodine resulted in a dramatic loss of potency (**26**). Replacement with an ethyl group (**27**) regained most of the activity while increasing the branching from isopropyl (**28**) to *t*-butyl (**29**) had minimal effect.

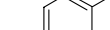
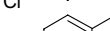
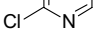
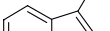
Replacing the iodo with chloro (**30**) resulted in a 3.6-fold loss of potency whereas the bromo analog (**31**) gave only a 2-fold decrease. Placing a chloro in the adjacent 8-position (**32**) showed an improvement relative to hydrogen, but this was not as good as chloro in the 7-position (**30**). Adding a chloro to the 8-position while retaining the 7-iodo-substituent (**33**) did not increase the potency additively.

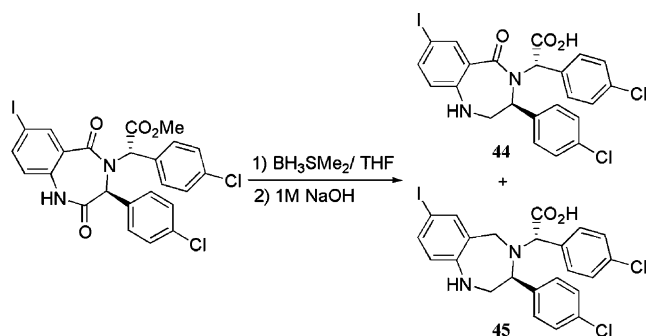
O=C1NC(=O)[C@H](c2ccc(Cl)cc2)N(C[C@@H](C(=O)O)c3ccc(Cl)cc3)C1=Cc4ccc(R)cc4

Compd	R	TF K_d (μ M)	FP IC ₅₀ (μ M)
20	7-I	0.067	0.42 \pm 0.02
26	7-H	7.69	14.8 \pm 0.5
27	7-CH ₂ CH ₃	—	1.5 \pm 0.2
28	7-CH(CH ₃) ₂	—	1.02 \pm 0.03
29	7-C(CH ₃) ₃	—	2.27 \pm 0.09
30	7-Cl	0.83	1.53 \pm 0.08
31	7-Br	0.83	0.97 \pm 0.11
32	8-Cl	1.67	6.3 \pm 0.4
33	7-I,8-Cl	0.167	0.70 \pm 0.04
34	7-CH ₂ OH	—	3.3 \pm 0.3
35	7-CH ₂ CH ₂ OH	—	2.4 \pm 0.3
36	7-NHAc	—	>125
37	7-CN	10.0	14.8 \pm 0.4
38	7-C \equiv CH	0.25	0.87 \pm 0.05

A 3D molecular model showing a ligand (represented by a stick model with purple and yellow atoms) bound within the binding pocket of a protein. The protein's surface is colored green, red, and blue, indicating different chemical environments. The ligand is positioned within the pocket, interacting with the protein's residues.

O=C1NC(=O)C2=CC=C(C=C2C1=O)C(=O)N(C2=CC=C(C=C2)C(=O)O)C3=CC=C(C=C3)C(=O)O

Compd	R	X	FP IC ₅₀ (μM)
40		N	1.47 ± 0.21
41		CH	7.4 ± 0.9
42		CH	55 ± 2
43		CH	7.9 ± 0.9



Scheme 2. Reduction of the BDP ring.

The indole NH of **43** may have the correct trajectory and N–O distance for hydrogen bonding, but according to the model, the indole is thrust deeper into the pocket than Trp-23. This may result in a potential clash with the pocket floor. The observed potency suggests that this substituent is indeed too large for the binding site (Table 4).

Since the chiral centers of the BDP epimerized under the basic conditions used to saponify the esters, the reduction of the adjacent amide carbonyl was performed (Scheme 2). The ester of **20** was treated with borane–methyl sulfide in THF resulting in reduction of the mono-substituted amide as the major product; however, over-reduction was also observed. Separation of the products followed by hydrolysis gave **44** and **45**. The activity of **44** and **45** in the FP assay were 0.49 ± 0.02 and $>125 \mu\text{M}$, respectively, thus **44** is essentially equipotent with **20** while **45** is inactive. This result is consistent with conformational analyses that suggest that the active BDP conformation remains reasonably accessible with removal of one of the amide groups, whereas removal of both yields a highly flexible molecule for which the required conformation is relatively inaccessible.²²

In conclusion, the use of ThermoFluor® screening technology in combination with a secondary FP assay led to the discovery and rapid optimization of potent 1,4-benzodiazepine-2,5-dione antagonists of the p53–HDM2 interaction. The most potent antagonists possessed chlorophenyl substituents that occupy two of the three hydrophobic pockets and an iodo group filling the third, as exemplified by **20** and **44**. A binding model was predicted on the basis of conformational analysis and the published structure of a peptide complex. This model was later confirmed by a BDP–HDM2 co-crystal structure.²⁶ Cell-based activity and structural information of the BDP–HDM2 complex are reported elsewhere.²⁶ Analogs of this series are being further developed and evaluated utilizing in vivo models.

Acknowledgements

The authors thank Michael X. Kolpak and Karen DiLoreto for their assistance in running NMR and LCMS experiments.

References and notes

- Fridman, J. S.; Lowe, S. W. *Oncogene* **2003**, *22*, 9030.
- Soussi, T.; Dehouche, K.; Beroud, C. *Hum. Mutat.* **2000**, *21*, 105.
- Eymin, B.; Gazzeri, S.; Brambilla, C.; Brambilla, E. *Oncogene* **2002**, *2*, 2750.
- Polsky, D.; Bastian, B. C.; Hazan, C.; Melzer, K.; Pack, J.; Houghton, A.; Busam, K.; Cordon-Cardo, C.; Osam, I. *Cancer Res.* **2001**, *2*, 7642.
- Momand, J.; Jung, D.; Wilczynski, S.; Niland, J. *Nucleic Acids Res.* **1998**, *26*, 3453.
- Iwakuma, T.; Lozano, G. *Mol. Cancer Res.* **2003**, *1*, 993.
- García-Echeverría, C.; Chène, P.; Blommers, M. J. J.; Furet, P. *J. Med. Chem.* **2000**, *43*, 3205.
- Stoll, R.; Renner, C.; Hansen, S.; Palme, S.; Klein, C.; Belling, A.; Zeslawski, W.; Kamionka, M.; Rehm, T.; Muhlhahn, P.; Schumacher, R.; Hesse, F.; Kaluza, B.; Voelter, W.; Engh, R. A.; Holak, T. A. *Biochemistry* **2001**, *40*, 336.
- Zhao, J.; Wang, M.; Chen, J.; Luo, A.; Wang, X.; Wu, M.; Yin, D.; Liu, Z. *Cancer Lett.* **2002**, *183*, 69.
- Galatin, P. S.; Abraham, D. J. *J. Med. Chem.* **2004**, *47*, 4163.
- Kritzer, J. A.; Lear, J. D.; Hodsdon, M. E.; Schepartz, A. *J. Am. Chem. Soc.* **2004**, *126*, 9468.
- Vassilev, L. T.; Vu, B. T.; Graves, B.; Carvajal, D.; Podlaski, F.; Filipovic, Z.; Kong, N.; Kammlott, U.; Lukacs, C.; Klein, C.; Fotouhi, N.; Liu, E. A. *Science* **2004**, *303*, 844.
- Zhang, R.; Mayhood, T.; Lipari, P.; Wang, Y.; Durkin, J.; Syto, R.; Gesell, J.; McNemar, C.; Windsor, W. *Anal. Biochem.* **2004**, *331*, 138.
- Agrafiotis, D. K.; Lobanov, V. S.; Salemme, F. R. *Nat. Rev. Drug Discovery* **2002**, *1*, 337.
- Agrafiotis, D. K. *J. Chem. Inf. Comput. Sci.* **1997**, *37*, 841.
- Rassokhin, D. N.; Agrafiotis, D. K. *J. Mol. Graph. Model.* **2000**, *18*, 370.
- Gokel, G.; Lüdke, G.; Ugi, I. In *Isonitrile Chemistry*; Ugi, I., Ed.; Academic: New York, 1971; p 145.
- Hulme, C.; Peng, J.; Tang, S.-Y.; Burns, C. J.; Morize, I.; Labaudiniere, R. *J. Org. Chem.* **1998**, *63*, 8021.
- Keating, T. A.; Armstrong, R. W. *J. Am. Chem. Soc.* **1996**, *118*, 2574.
- Pantoliano, M. W.; Petrella, E. C.; Kwasnoski, J. D.; Lobanov, V. S.; Myslik, J.; Graf, E.; Carver, T.; Asel, E.; Springer, B. A.; Lane, P.; Salemme, F. R. *J. Biomol. Screen.* **2001**, *6*, 429.
- Typical FP assay conditions were as follows: 20 nM HDM2 (17–125), 5 nM fluorescein-labeled p53-derived 9-mer peptide (N-terminal fluorescein-RFMDYWEGL, $K_d = 20 \text{ nM}$), 50 mM Hepes pH 7.5, 150 mM NaCl, 3 mM β -octyl glucopyranoside, and 2.5% DMSO. Compound, HDM2 and peptide were incubated for 15–20 min at room temperature prior to reading the fluorescence polarization (excitation = 485 nm, emission = 530 nm).
- Unpublished results.
- Cognate Preparation*. DL-2-Aminophenylacetic Acid, 5th ed. In *Vogel's Textbook of Practical Organic Chemistry*; Furniss, B. S.; Hannaford, A. J.; Smith, P. W. G., Tatchell, A. R., Eds.; John Wiley & Sons: New York, 1989; p 754.
- Kussie, P. H.; Gorina, S.; Marechal, V.; Elenbaas, B.; Moreau, J.; Levine, A. J.; Pavletich, N. P. *Science* **1996**, *274*, 948.
- Calculated using Chemdraw Ultra® Version 6.0.2, CambridgeSoft.com, Cambridge Park Drive, Cambridge, MA 02140.

26. Grasberger, B. L.; Lu, T.; Schubert, C.; Parks, D. J.; Carver, T. E.; Koblish, H. K.; Cummings, M. D.; LaFrance, L. V.; Milkiewicz, K. L.; Calvo, R. R.; Maguire, D.; Lattanze, J.; Franks, C. F.; Zhao, S-Y.; Ramachandren, K.; Bylebyl, G. R.; Zhang, M.; Manthey, C. L.; Petrella, E. C.; Pantoliano, M. W.; Deckman, I. C.; Spurlino, J. C.; Maroney, A. C.; Tomczuk, B. E.; Molloy, C. J.; Bone, R. F. *J. Med. Chem.*, submitted for publication.